Rare Met. (2014) 33(6):761–766
DOI 10.1007/s12598-013-0150-x

RARE METALS
www.editorialmanager.com/rmet

Inclusions and solidification structures of high pure ferritic stainless steels dual stabilized by niobium and titanium

Hong-Po Wang, Li-Feng Sun*, Jun-Jie Shi, Cheng-Jun Liu, Mao-Fa Jiang, Chi Zhang

Received: 26 October 2012 / Revised: 1 April 2013 / Accepted: 20 April 2013 / Published online: 24 October 2013

Abstract As the raw materials in the post process of rolling and heat treatment, ingots have great effects on the properties of the final products. Inclusions and solidification structures are the most important aspects of the quality of ingots. Niobium and titanium are usually used to react with carbon and nitrogen to improve the properties of ferritic stainless steels. In this research, combined with thermodynamic calculation, effects of niobium and titanium on the inclusions and solidification structures in three kinds of high pure ferritic stainless steels with different titanium additions were investigated by optical microscope (OM), scanning electron microscope (SEM), transmission electron microscope (TEM), and energy disperse spectrometer (EDS). Results show that Al_2O_3 and a few (Nb,Ti)N particles form when titanium addition is 0.01 %. Furthermore, inclusions are mainly TiN and Al_2O_3–TiO_x–TiN duplex inclusions when titanium addition is more than 0.10 %. Those two types of inclusions are in well distribution, and can afford nuclei to the solidification process. Therefore, the ratio of equiaxed zone increases with the increase of titanium addition. The ratio increases from 42.1 % to 64.0 % with the titanium addition increasing from 0.01 % to 0.10 %, and it increases to 85.7 % when the titanium addition reaches 0.34 %.

H.-P. Wang, L.-F. Sun*, J.-J. Shi, C.-J. Liu, M.-F. Jiang, C. Zhang
Key Laboratory for Ecological Metallurgy of Multimetallic Ores (Ministry of Education), Northeastern University, Shenyang 110819, China
e-mail: sunlf@smm.neu.edu.cn

H.-P. Wang
e-mail: whp_neu@163.com

Keywords High pure ferritic stainless steel; Inclusion; Solidification structure; Equiaxed zone; Stabilization element

1 Introduction

Ferritic stainless steels are widely used in manufacturing, construction industry, and sanitary tools because of their perfect mechanical properties and corrosion resistance [1–3]. As the raw materials in the post process of rolling and heat treatment, the solidification structures of the ingots have great effects on the recrystallization microstructure, texture, and formability of their final products [4–8]. Solidification structures are determined by many factors, such as chemical compositions, superheat, quantity of cooling water, and casting speed [9–12]. Niobium and titanium are usually added into high pure ferritic stainless steels as stabilization elements to react with carbon and nitrogen to promote their mechanical properties and corrosion resistance [13]. Moreover, the nitrides of titanium and niobium can be used as nuclei for the solidification process so as to refine the solidification structures and increase the ratio of equiaxed zone.

In the past two decades, researches on the inclusions and solidification structures of ferritic stainless steels were mainly focused on traditional SUS430 steel or the ones without stabilizing elements. In recent years, high pure ferritic stainless steels with a total content of carbon and nitrogen less than 300×10^{-6} were developed as the substitutes for SUS304 stainless steels. And there are few studies concentrated on the high pure ones with high chromium content and dual stabilized by niobium and titanium. Therefore, the aim of this study is to determine the effect of niobium and titanium on the inclusions and

solidification structures of high pure ferritic stainless steels. Combined with thermodynamic calculation, the inclusions formed in or before the solidification process and their effects on the solidification structures of three kinds of these steels with 21 % chromium were investigated.

2 Experimental

The raw materials were prepared by vacuum induction furnace using various alloys. 110 kg ingot for each kind of the steel was obtained. Table 1 shows the chemical compositions of the raw materials.

The samples used to observe solidification structures with the size of 80 mm × 20 mm × 20 mm were taken from the middle of ingots, as shown in Fig. 1a. After polished by emery paper and polishing machine, the samples were etched by the corrosive solution consisting of 10 g iron trichloride, 30 ml hydrochloric acid, and 120 ml deionized water. Finally, high resolution scanner was used to scan the surfaces of the samples. Additionally, some specimens with the size of 20 mm × 20 mm × 20 mm used to observe inclusions were taken from the position of half radius at the cross section of the ingots, as shown in Fig. 1b. The inclusions were investigated by optical microscope (OM), scanning electron microscope (SEM), transmission electron microscope (TEM), and energy dispersive spectrometer (EDS).

3 Results and discussion

3.1 Types of inclusions

Experiment results show that the inclusions in the ingots of the three steels are mainly TiN, Al_2O_3, Al_2O_3–TiO_x–TiN, and a few (Nb,Ti)N inclusions. Statistical analysis on the types of the inclusions was carried out by OM, SEM, and EDS, as shown in Table 2.

Al_2O_3 forms at a high temperature even at 1,600 °C because it has a very low solubility product. Researchers made plenty of work on the formation of Al_2O_3. Therefore, the precipitation process of inclusions in the present work mainly focused on the inclusions containing titanium and niobium.

Figure 2 shows the shape and EDS analysis of TiN precipitates. Their sizes are in the range of 1–10 μm. Since the solubility product of AlN is higher than TiN by 2–3 orders of magnitude in the range of 900–1,500 °C and titanium has a strong ability to react with nitrogen [14]. It can be assumed that all nitrogen react with titanium. The minimum additions of titanium for steel No. 1, No. 2, and No. 3 were calculated to be 0.028 %, 0.030 %, and 0.032 %, respectively. Obviously, 0.01 % Ti addition in steel No. 1 is far from enough to react with the total nitrogen. Therefore, the excess nitrogen would react with niobium to form NbN. As a result, NbN would be combined with TiN and then (Ti,Nb)N precipitates form [15], which is found in steel No. 1, as shown in Fig. 3.

Table 1 Chemical compositions of raw materials (wt%)

Nos.	C	Si	Mn	Cr	N	Ti	Nb	T.Al	T.O
1	0.010	0.45	0.16	21.21	0.0082	0.01	0.28	0.010	0.0098
2	0.012	0.51	0.12	21.23	0.0086	0.10	0.27	0.018	0.0055
3	0.012	0.47	0.18	21.35	0.0093	0.34	0.28	0.021	0.0059

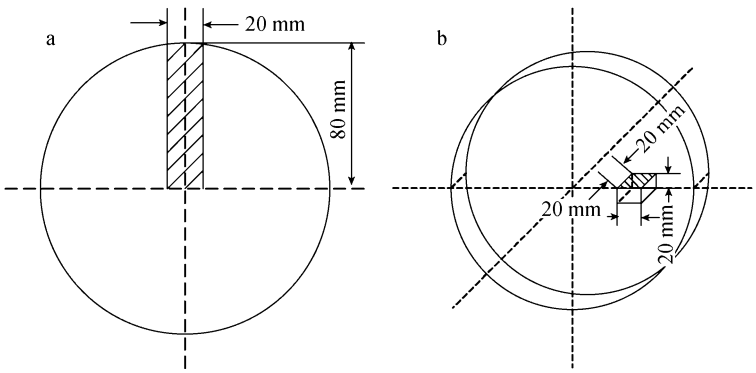

Fig. 1 Diagrams of sampling positions at the cross section of the ingots: **a** solidification structure observation and **b** inclusion observation

Table 2 Inclusion types in ingots

Nos.	Types of inclusions
1	Al_2O_3, a few (Nb,Ti)N
2	Al_2O_3–TiO_x–TiN, TiN
3	Al_2O_3–TiO_x–TiN, a lot of TiN

Figure 4 shows the shape and EDS analysis of Al_2O_3–TiO_x–TiN duplex inclusions. This type of inclusion is only found in steel No. 2 and No. 3. The cores of these inclusions are Al_2O_3–TiO_x and covered with TiN. It is obviously concluded that TiN forms after Al_2O_3 and TiO_x, which is in good accordance with the previous researches [16, 17]. Additionally, these inclusions do not form in steel No. 1 because the titanium addition is too low to form TiN in or before the solidification process. Thus, the inclusions in steel No. 1 are mainly pure Al_2O_3.

3.2 Precipitation process of inclusions containing titanium

Inclusions containing titanium are mainly TiN in the present work. TiN forms at a high temperature even higher than the liquidus temperature of steel because of the strong reaction ability between titanium and nitrogen. Equation (1) shows the reaction between [Ti] and [N] and its standard Gibbs free energy [18]. Taking 1 % solution as the standard state, relations between the product of %[Ti]·%[N] and temperature were obtained by calculating the activity coefficients f_{Ti} and f_N, as shown in Eq. (2). K is the equilibrium constant. Figure 5 demonstrates the solubility diagram of TiN. Besides, the liquidus temperatures of steel No. 1, No. 2, and No. 3 were calculated to be 1,496.2, 1,495.2, and 1,495.4 °C, respectively, according to Eq. (3) [19].

$$[\mathrm{Ti}] + [\mathrm{N}] = \mathrm{TiN(s)}\ \Delta G^{\mathrm{o}} = -314800 + 114.35\,T \quad (1)$$

$$\%[\mathrm{Ti}]\cdot\%[\mathrm{N}] = 1/(K \cdot f_{\mathrm{Ti}} \cdot f_{\mathrm{N}}) \quad (2)$$

$$T = 1536 - \{0.1 + 83.9[\mathrm{C}] + 10[\mathrm{C}]^2 + 12.6[\mathrm{Si}] + 5.4[\mathrm{Mn}] + 4.6[\mathrm{Cu}] + 5.1[\mathrm{Ni}] + 1.5[\mathrm{Cr}] - 30[\mathrm{P}] - 37[\mathrm{S}] - 9.5[\mathrm{Nb}]\} \quad (3)$$

Calculated results show that TiN does not start to form before the process of solidification in steel No. 1 and No. 2, but it starts in steel No. 3. In addition, some titanium oxides form as the cores of Al_2O_3–TiO_x–TiN duplex inclusions in all the three kinds of the steels. Previous researches show that titanium oxides are mainly Ti_2O_3 when titanium content is higher than 0.25 % and changes into Ti_3O_5 when titanium content is lower than 0.25 % [20, 21]. The precipitation temperatures of TiN would be a little lower than the

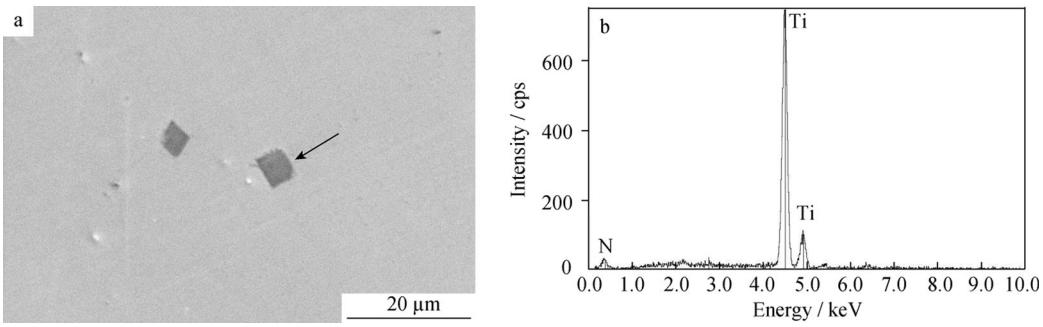

Fig. 2 SEM image **a** and EDS analysis **b** of TiN particle

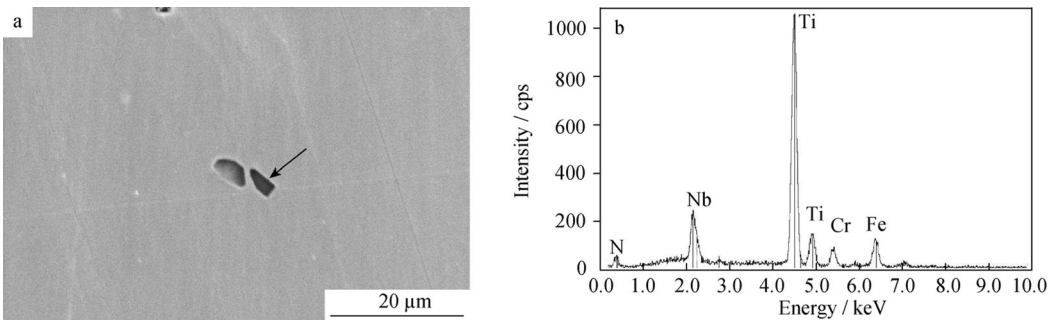

Fig. 3 SEM image **a** and EDS analysis **b** of (Nb,Ti)N particles

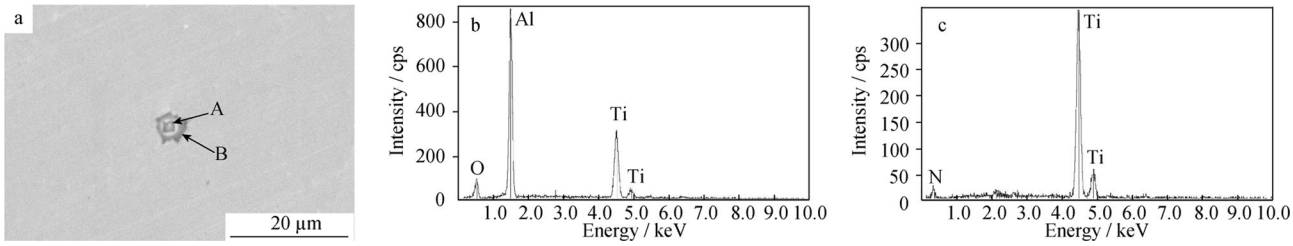

Fig. 4 SEM image **a** and EDS analysis of Al_2O_3–TiO_x–TiN duplex inclusions: **b** A in **a**, **c** B in **a**

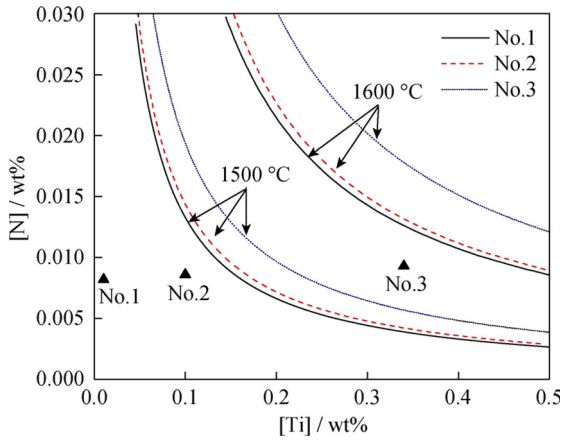

Fig. 5 Solubility diagram of TiN

calculated values because of the formation of titanium oxides, but the tendency that the precipitation temperature rises with the titanium addition increasing would not change.

3.3 Precipitation process of inclusions containing niobium

Under this experimental condition, the inclusions containing niobium are carbonitrides. Reactions among niobium, carbon, and nitrogen are shown in Eqs. (4) to (5) [22–24]. Assumed that all niobium react with carbon, the full solution temperatures of NbC for steel No. 1, No. 2, and No. 3 are calculated to be 1,100, 1,111, and 1,114 °C, respectively. Assumed that all niobium react with nitrogen, the full solution temperatures of NbN for steel No. 1, No. 2, and No. 3 are calculated to be 1,350, 1,351, and 1,361 °C, respectively. It reveals that both NbC and NbN would not form until the solidification is totally finished. However, Nb(C,N) may form because NbN is mutually soluble with NbC and the solution temperature of Nb(C,N) is higher than that of NbN or NbC [25]. Experiment results show that there are actually a few TiN particles containing niobium carbonitrides in steel No. 1. And these carbonitrides are mainly NbN since there is not enough titanium to consume all the nitrogen.

$$\lg([\mathrm{Nb}]\cdot[\mathrm{C}]) = 5.43 - 10960/T, \quad (4)$$

$$\lg([\mathrm{Nb}]\cdot[\mathrm{N}]) = 4.96 - 12330/T. \quad (5)$$

However, most of nitrogen would react with titanium so that the full solution temperatures of Nb(C,N) and NbN are lower than the calculated values for steel No. 2 and No. 3. Therefore, the carbonitrides of niobium would mainly precipitate in the process of rolling and annealing. Experiment results show that there are a lot of NbC particles with the size less than 500 nm in cold-rolled sheet, as shown in Fig. 6.

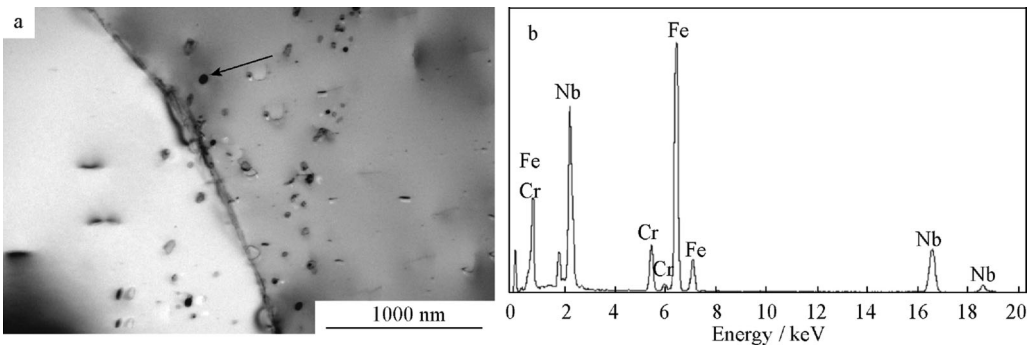

Fig. 6 NbC particles in annealed cold-rolled sheet: **a** SEM image and **b** EDS analysis

3.4 Effect of niobium and titanium additions on solidification structures

Figures 7 and 8 show the solidification structures and the ratios of equiaxed zone of the ingots. It shows that the ratios of equiaxed zone increase with the titanium addition increasing, which is related with the inclusions and their distributions. Al_2O_3 forms at a high temperature and is in non-uniform distribution, as shown in Fig. 9a. Steel No. 1 has the lowest ratio of equiaxed zone, because there are only a few (Nb,Ti)N particles. Although there are some Al_2O_3 particles in steel No. 1, pure Al_2O_3 particles are not in well distribution and only have a weak effect on the solidification structures.

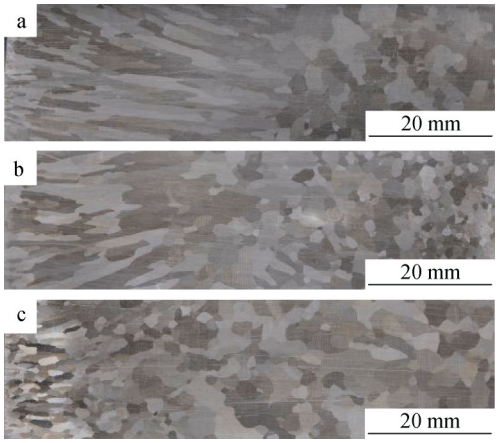

Fig. 7 Solidification structures at cross sections of ingots: **a** steel No. 1, **b** steel No. 2, and **c** steel No. 3 (Left side being surface of the ingots and right side being the center)

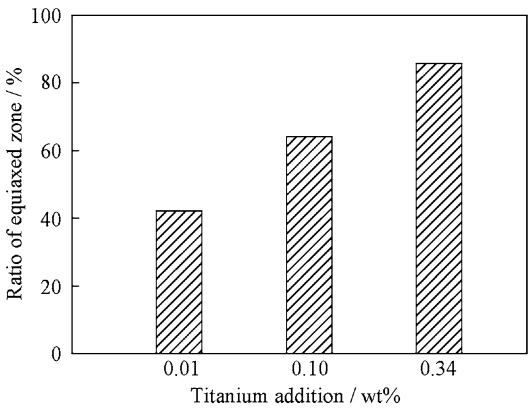

Fig. 8 Ratios of equiaxed zone of the ingots with different titanium additions

Figure 9b shows the inclusion distributions of the ingots in steel No. 3. Those inclusions were mostly determined to be TiN and Al_2O_3–TiO_x–TiN by EDS. And they are in well distribution. Figure 8 shows the ratio of equiaxed zone in solidification structures increases with the titanium addition increasing. The ratio increases from 42.1 % to 64.0 % with the titanium addition increasing from 0.01 % to 0.10 %, and it increases to 85.7 % when the titanium addition reaches 0.34 %. It is concluded that well-distributed TiN and Al_2O_3–TiO_x–TiN particles form in the process of melting and solidification could effectively afford nuclei to make liquid steel solidify in a relatively big zone at the same time, which promotes the ratio of equiaxed zone.

Besides, there are about 0.28 % Nb in all the three high pure ferritic stainless steels in the present work, but it has little effect on the ratio of equiaxed zone because the inclusions containing niobium mainly form after the solidification process.

4 Conclusion

As stabilization elements added into high pure ferritic stainless steels, titanium has great effect on the precipitation of inclusions and solidification structures. There are mainly two kinds of inclusions, which are TiN and Al_2O_3–TiO_x–TiN. They are of benefit to improve the ratio of equiaxed zone. The ratio increases from 42.1 % to 64.0 % with the titanium addition increasing from 0.01 % to 0.10 % and increases to 85.7 % when the titanium addition reaches 0.34 %.

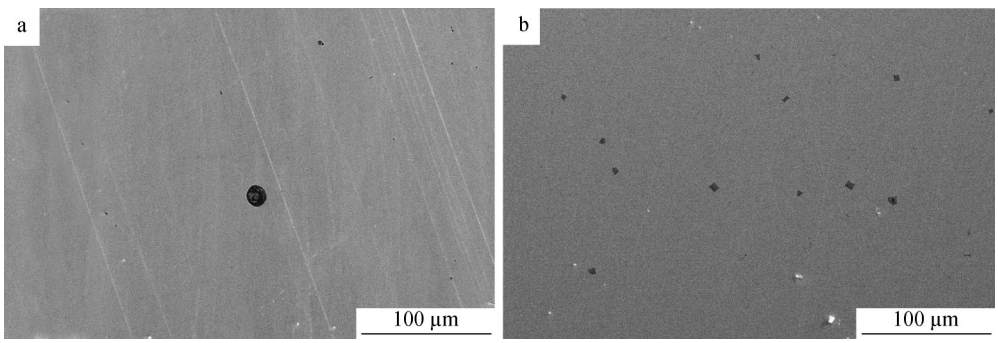

Fig. 9 SEM images of inclusion distributions in ingots: **a** steel No. 1 and **b** steel No. 3

Effect of titanium on the solidification structure is far stronger than that of niobium. Only a few (Nb,Ti)N particles would form in the solidification process and have a certain effect on the solidification structures, when there is not enough titanium to consume the total nitrogen. Most of the inclusions containing niobium form after solidification.

Acknowledgments This study was financially supported by the Fundamental Research Funds for the Central Universities (No. N100602011), the National Natural Science Foundation of China (No. 51104039), the National Key Basic Research Program of China (No. 2012CB626812), the Program for New Century Excellent Talents in University (No. NCET-11-0077), Liaoning Provincial Natural Science Foundation of China (No. 201102062), Liaoning Provincial Science and Technology Plan (No. 2012221013), and the National Innovation Experiment Program for University Students.

References

[1] Gardner L. The use of stainless steel in structures. Progress Struct Eng Mater. 2005;7(2):45.
[2] Kim JK, Kim YH, Uhm SH, Lee JS, Kim KY. Intergranular corrosion of Ti-stabilized 11 wt% Cr ferritic stainless steel for automotive exhaust systems. Corro Sci. 2009;51(11):2716.
[3] Fujita N, Kikuchi M, Ohmura K, Suzuki T, Funaki S, Hiroshige I. Effect of Nb on high-temperature properties for ferritic stainless steel. Scripta Mater. 1996;35(6):705.
[4] Du W, Jiang L, Sun Q, Yu H, Qin B, Liu Z. Effect of the solidification structure on the ridging and drawability of ultra low carbon ferritic stainless steel. Baosteel Tech Res. 2010;4(1):35.
[5] Hamada J, Matsumoto Y, Fudanoki F, Maeda S. Effect of initial solidified structure on ridging phenomenon and texture in type 430 ferritic stainless steel sheets. ISIJ Int. 2003;43(12):1989.
[6] Yazawa Y, Ozaki Y, Kato Y, Furukimi O. Development of ferritic stainless steel sheets with excellent deep drawability by 111 recrystallization texture control. Jsae Rev. 2003;24(4):483.
[7] Liu H, Du W, Xie S, Liu Z, Wang G. The effect of initial solidification structure on ridging in Cr17 ferritic stainless steels. Chin J Mater Res. 2008;22(5):467.
[8] Liu H, Du W, Xie S, Liu Z, Wang G. Effects of initial solidification structure on microstructure, texture and formability of Cr17 ferritic stainless steel. J Iron Steel Res. 2008;20(10):32.
[9] Li J, Jie W, Yang G, Zhou Y. Solidification structure formation in undercooled Fe-Ni alloy. Acta Mater. 2002;50(7):1797.
[10] Ozbayraktar S, Koursaris A. Effect of superheat on the solidification structures of AISI 310S austenitic stainless steel. Metall Mater Trans B. 1996;27(2):287.
[11] Liu C, Wang H, Jiang M. Research on solidification structure of billet for bearing steel. Rare Metal Mat Eng. 2011;40(S3):220.
[12] Suito H, Ohta H, Morioka S. Refinement of solidification microstructure and austenite grain by fine inclusion particles. ISIJ Int. 2006;46(6):840.
[13] Gordon W, Van Bennekom A. Review of stabilisation of ferritic stainless steels. Mater Sci Tech. 1996;12(2):126.
[14] Suzuki S, Weatherly GC, Houghton DC. The response of carbonitride particles in hsla steels to weld thermal cycles. Acta Metall. 1987;35(2):341.
[15] Hua M, Garcia CI, DeArdo AJ. Precipitation behavior in ultra-low-carbon steels containing titanium and niobium. Metall Mater Trans A. 1997;28(9):1769.
[16] Ma Z, Janke D. Characteristics of oxide precipitation and growth during solidification of deoxidized steel. ISIJ Int. 1998; 38(1):46.
[17] Xia W, Wang Y, Wang M, Shengtao Q. Behavior of oxide precipitation in solidification process for alumium-titanium deoxidized steels. J Iron Steel Res. 2011;23(8):11.
[18] Liang Y, Che Y. Thermodynamic Data Notebook of Inorganics. Shenyang: Northeast University Press; 1993. 505.
[19] Wu Y, Jiang Z, Liang L, Maofa J, Yang L. Calculation on liquidus temperature of steel. J Iron Steel Res. 2002;14(6):6.
[20] Cha WY, Nagasaka T, Miki T, Sasaki Y, Hino M. Equilibrium between titanium and oxygen in liquid Fe–Ti alloy coexisted with titanium oxides at 1873 K. ISIJ Int. 2006;46(7):996.
[21] Pak JJ, Jo JO, Kim SI, Kim WY, Chung TI, Seo SM, Park JH, Kim DS. Thermodynamics of titanium and oxygen dissolved in liquid iron equilibrated with titanium oxides. ISIJ Int. 2007; 47(1):16.
[22] Taylor KA. Solubility products for titanium-, vanadium-, and niobium-carbide in ferrite. Scripta Metall Mater. 1995;32(1):7.
[23] Matsuda S, Okumura N. Effect of distribution of Ti nitride precipitate particles on the austenite grain size of low carbon and low alloy steels. Trans ISIJ. 1978;18(4):198.
[24] Narita K. Physical chemistry of the groups IVa (Ti, Zr), Va (V, Nb, Ta) and the rare earth elements in steel. Trans ISIJ. 1975; 15:145.
[25] Yong Q. Secondary Phases in Steels. Beijing: Metallurgical Industry Press; 2006. 173.